

Flux and fluence effects on the Vacuum-UV photodesorption and photoprocessing of CO₂ ices

– Electronic Supplementary Information –

Antoine Hacquard, Daniela Torres-Diaz, Romain Basalgète, Delfina Toulouse, Géraldine Féraud, Samuel Del Fré, Jennifer A. Noble, Laurent Philippe, Xavier Michaut, Jean-Hugues Fillion, Anne Lafosse, Lionel Amiaud and Mathieu Bertin

A- Temperature Programmed Desorption and estimation of ice composition after irradiation

Temperature Programmed Desorption (TPD) consists in applying a constant heating ramp to the sample and monitoring the desorbed species as a function of the sample temperature by means of a quadrupole mass spectrometer (QMS). In our study, TPD has been mainly used to estimate the chemical composition of the ice after each irradiation, by integrating the thermal desorption signals of each mass, which is directly proportional to the total amount of adsorbed molecules before the warming-up. Figure A1 shows the TPD curves performed from pure CO₂ ices after their irradiation by 12 eV photons. Three mass channels were monitored, namely mass 44 u (CO₂⁺), 28 u (CO⁺) and 32 u (O₂⁺). Masses 44 u and 32 u can only be associated with the desorption of CO₂ and O₂ respectively. Mass 28 u, on the other hand, is associated with both the desorption of CO, and the dissociative electron impact ionization of the CO₂ in the ionization chamber of the QMS. The clear desorption of both O₂ and CO, both at low temperature and with the CO₂ desorption, clearly indicates their presence on and in the ice due to the irradiation. By correcting the TPD integrated signal of 28 u using (i) the mass-dependent apparatus function of the QMS, (ii) the ionization cross sections of CO and (iii) the correction of the part of the signal due to the cracking of CO₂, one can estimate the total amount of CO in the ice after irradiation, accounting to 20 % of the total of the remaining molecules after irradiation. The fraction of other species, such as O₂ (shown), were found comparatively negligible. In order to further validate this estimation, a TPD of prepared CO:CO₂ mixed ice, in which CO represented 20 % of the deposited molecules, was performed in the same conditions. The resulting TPD is shown in the fig. A2, and compares very well to the TPD obtained after the irradiation of the pure CO₂ ice.

B- Single exponential fitting to probe the evolutions of the desorption and of the chemical composition of the ice with photon fluence

Single exponential fits were done in order to investigate the different kinetics observed in the photodesorption yields and in the integrated absorbance band of CO, both as a function of photon fluence. Though only the cross sections were indicated in the main text, we present in Table B1 all the other fitting parameters obtained from fits using eq. (3), (4) and (5).

C- Additional experiments to probe the ice structure and particularly the crystallinity

We have performed additional experiments aiming to study ice structure, in particular crystallinity. We have grown a crystalline CO₂ ices by depositing it at 50K, following the protocol suggested in Tsuge et al. 2020. The procedure is to cool down the ice to 16K once the crystalline ice has grown on the sample holder. The profile of the CO₂ asymmetric stretching mode was definitely not the same as presented in the manuscript (red curve here), which gives us further confidence that our sample was not crystalline. Indeed, RAIRS spectra of the crystalline CO₂ ice

presented here highlights a particular band profile. Intensity of the feature corresponding to the TO mode is higher than one of the amorphous ices presented in our study. Furthermore, the intensity ratio between the LO and TO mode is inverted, LO mode being predominant in the amorphous ice in our set-up geometry.

Photodesorption evolution asymptotic value for species	Flux (photon/s/cm ²)		
	7.3×10^{12}	1.3×10^{14}	2.2×10^{14}
$\Gamma_{\infty}(\text{CO}_2)$	$1.0 \pm 2.0 \times 10^{-4}$	$4.6 \pm 0.1 \times 10^{-4}$	$4.4 \pm 0.1 \times 10^{-4}$
$\Gamma_{\infty}(\text{CO})$	$9.1 \pm 0.1 \times 10^{-3}$	$4.1 \pm 0.1 \times 10^{-3}$	$6.1 \pm 0.1 \times 10^{-3}$
$\Gamma_{\infty}(\text{O}_2)$	$2.7 \pm 0.1 \times 10^{-3}$	$1.2 \pm 0.1 \times 10^{-3}$	$1.5 \pm 0.1 \times 10^{-3}$
a_{CO}^{∞}	/	$8.9 \pm 0.2 \times 10^{-2}$	$7.7 \pm 0.9 \times 10^{-2}$

Table B1 – Asymptotic values used as fitting parameters. 50 ML of pure CO₂ ices were irradiated with different photon flux at 12 eV, values precised in the table. Γ_{∞} are obtained from eq. 3 for CO₂ and eq. 4, for CO and O₂; a_{CO}^{∞} is obtained from eq. 5.

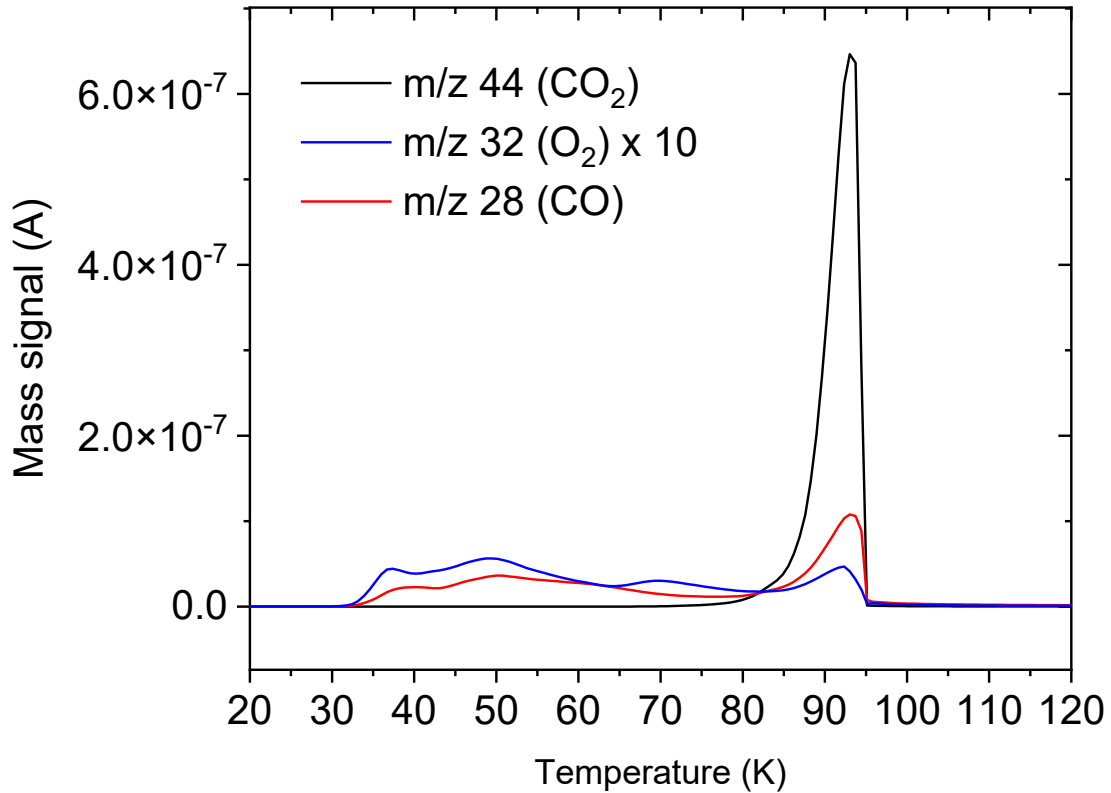


Figure A1 – TPD curves from 50 ML of CO₂ pure ice with an heating ramp of 12 K/min, after irradiation with 12 eV photons and with a photon flux of 2.2×10^{14} photon/s/cm². The total fluence was about 10^{18} cm⁻². Black line represents m/z 44, red line represents m/z 28 and blue line represent m/z 32, signal of mass 32 have been multiply per 10 for a better clarity.

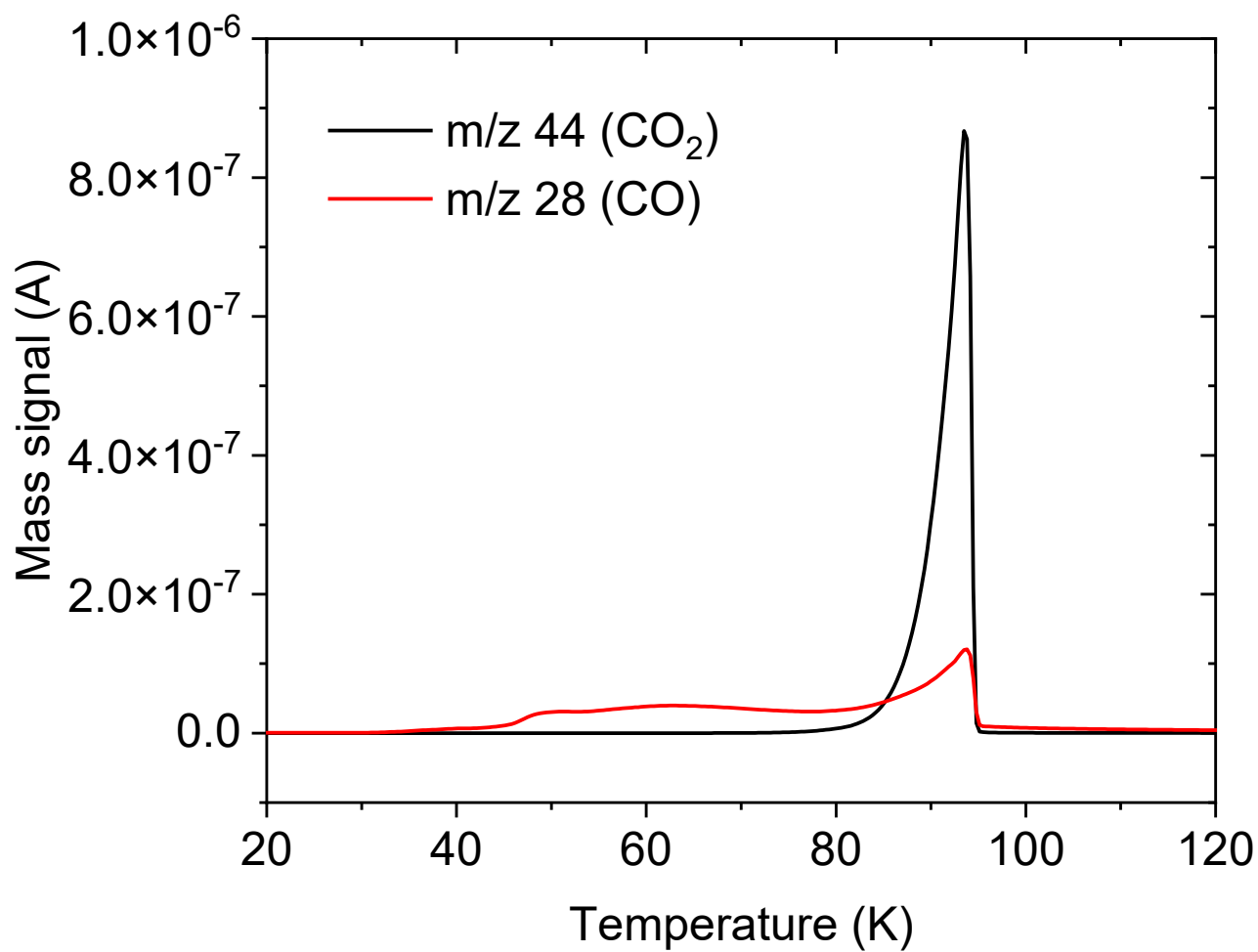


Figure A2 - TPD curves from a mixed CO:CO₂ ice with an heating ramp of 12 K/min, Proportion of CO in the mixed ice represent 20%. Black line represents m/z 44 , red line represents m/z 28.

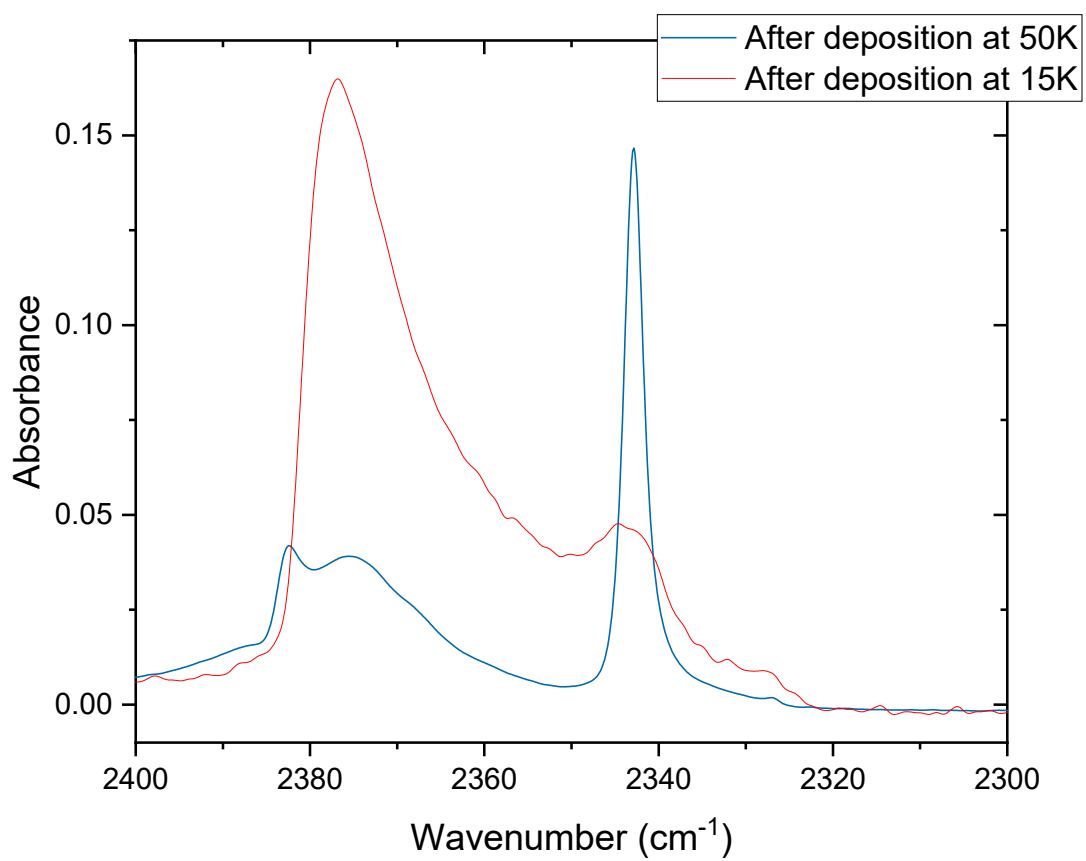


Figure C1 – RAIRS Spectra of the CO₂ stretching mode: after deposition of 20 ML of CO₂ pure ice at 50K (in blue) and after deposition of 50 ML of CO₂ pure ice at 15K (in red).